Community structural differences shape microbial responses to high molecular weight organic matter

John Paul Balmonte [1*†] Andrew Buckley,[1‡] Adrienne Hoarfrost,[1‡] Sherif Ghobrial,[1] Kai Ziervogel,[2] Andreas Teske[1] and Carol Arnosti[1]

[1]*Department of Marine Sciences, The University of North Carolina at Chapel Hill, Chapel Hill, NC 27599, USA.*

[2]*Institute for the Study of Earth, Oceans, and Space, University of New Hampshire, Durham, NH 03824, USA.*

Summary

The extent to which differences in microbial community structure result in variations in organic matter (OM) degradation is not well understood. Here, we tested the hypothesis that distinct marine microbial communities from North Atlantic surface and bottom waters would exhibit varying compositional succession and functional shifts in response to the same pool of complex high molecular weight (HMW-OM). We also hypothesized that microbial communities would produce a broader spectrum of enzymes upon exposure to HMW-OM, indicating a greater potential to degrade these compounds than reflected by initial enzymatic activities. Our results show that community succession in amended mesocosms was congruent with cell growth, increased bacterial production and most notably, with substantial shifts in enzymatic activities. In all amended mesocosms, closely related taxa that were initially rare became dominant at time frames during which a broader spectrum of active enzymes were detected compared to initial timepoints, indicating a similar response among different communities. However, succession on the whole-community level, and the rates, spectra and progression of enzymatic activities, reveal robust differences among distinct communities from discrete water masses. These results underscore the crucial role of rare bacterial taxa in ocean carbon cycling and the importance of bacterial community structure for HMW-OM degradation.

Received 14 June, 2018; revised 14 November, 2018; accepted 15 November, 2018. *For correspondence. E-mail jp.balmonte@gmail.com; Tel. +46-18-471-2725. †Present address: Department of Ecology and Genetics/Limnology, Uppsala University, Norbyvägen 18D, Uppsala 752 36, Sweden. ‡These authors contributed equally to this work.

Introduction

Marine microbial communities play a critical role in global carbon cycling by remineralizing an estimated half of the organic matter (OM) biosynthesized in the ocean (Azam and Malfatti, 2007). The initial step of OM degradation is catalysed by enzymes that hydrolyze high molecular weight (HMW) substrates. The enzymatic capabilities of microbial communities determine which constituents of OM are assimilated into biomass or remineralized, and which fractions evade degradation (Arnosti, 2011). Despite the global importance of microbially driven carbon cycling, constraining the factors that control the initial step of carbon cycling remains a challenge. For example, differences in rates and patterns of enzymatic hydrolysis – observed in multiple oceanic regions (Christian and Karl, 1995; Fukuda *et al.,* 2000; Arnosti, 2011) and at different depths (Davey *et al.,* 2001; Zaccone *et al.,* 2003; Baltar *et al.,* 2009; Hoarfrost and Arnosti, 2017) – may reflect variations in environmental factors, microbial community composition or both (Teske *et al.,* 2011; Balmonte *et al.,* 2018). This knowledge gap limits our understanding of the functional consequences of community composition, or structure–function relationships, for microbial degradation of OM, particularly for HMW compounds (Datta *et al.,* 2016; Enke *et al.,* 2018).

Microbial structure–function relationships can be characterized by functional dissimilarity or functional redundancy. In cases of functional dissimilarity, differences in microbial community composition can have consequences for function, independent of present environmental conditions (Reed and Martiny, 2007; Strickland *et al.,* 2009; Enke *et al.,* 2018). In contrast, communities are functionally redundant for ecosystem processes if certain functions can be performed by multiple microbial taxa (Louca *et al*., 2018); thus, differences in community structure may not necessarily yield variations in process rates, and environmental conditions ultimately govern specific functions of microbial communities (Langenheder *et al.,* 2006; Burke *et al.,* 2011; Frossard *et al.,* 2012; D'Ambrosio *et al.,* 2014). The balance between functional dissimilarity and functional redundancy within a community determines whether microbial responses to natural

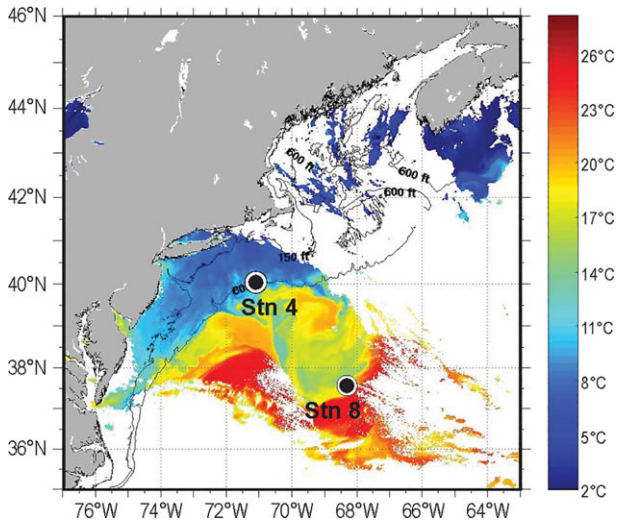

Fig. 1. Sampling stations in the North Atlantic.
The map was modified from the Rutgers Coastal Ocean Observation Lab, and shows NOAA-19 sea surface temperature data from April 29, 2015, 1834 GMT. White sections in the map denotes no sea surface temperature data are available.

environmental fluctuations or disturbances have functional implications (Allison and Martiny, 2008).

The phylogenetic range of specific functions within different microbial lineages, in part, determines the degree of functional redundancy within communities. For example, processes that are phylogenetically widespread, such as heterotrophic respiration, persist with little to no variation even with differences in community composition (Langenheder *et al.,* 2006). In contrast, functions that are confined to, or occur preferentially in specific groups – such as nitrogen fixation (Balser and Firestone, 2005; Bell *et al.,* 2005) or the ability to enzymatically hydrolyze specific compounds (Langenheder *et al.,* 2006) – show variable process rates with differences in community structure. In considering heterotrophy, the ability to utilize low molecular weight OM is more phylogenetically widespread than the ability to use specific HMW compounds (Logue *et al.,* 2016). The phylogenetic distribution of specific functions may be inversely correlated with the trait complexity – that is, functions that require a greater number of genes are carried out by fewer bacterial taxa (Martiny *et al.,* 2013). Thus, phylogenetic distribution of traits should be considered in investigations of structure–function relationships (Comte *et al.,* 2013; Knelman and Nemergut, 2014).

In the oceans, water masses are characterized by hydrographic signatures and corresponding microbial communities (Galand *et al.,* 2010; Agogue *et al.,* 2011), but whether community compositional differences in distinct water masses have consequences for OM degradation, especially for HMW compounds, is little understood. To address this question, we investigated the compositional and functional succession of distinct marine microbial communities from four different North Atlantic water masses, in response to the addition of high molecular weight OM (HMW-OM) derived from *Thalassiosira weissflogii*, a globally widespread centric diatom (Hartley *et al*., 1996; Stoermer, 1978). We tested the hypothesis of bacterial functional dissimilarity for the degradation of HMW-OM: distinct bacterial communities would exhibit varying compositional and enzymatic succession in response to the addition of a heterogeneous pool of HMW-OM, which will likely select for taxa with the ability to hydrolyze HMW substrates. We also hypothesized that, upon exposure to HMW-OM, microbial communities would produce a broader spectrum of enzymes, indicating a greater community potential to degrade these compounds than reflected by limited initial enzymatic activities. Exposing distinct microbial communities to the same HMW-OM addition in mesocosms provides insights into the consequences of community structural differences for HMW-OM degradation, as well as the identities of marine microbial taxa that play a role in this process.

Results

Water mass characteristics

Distinct water masses were sampled for the mesocosm experiments (Fig. 1; Supporting Information Fig. S1; see Experimental Procedures). Hydrographic conditions differed at the surface and bottom waters of Stns 4 and 8, which were located on the continental shelf and in the open ocean, respectively (Fig. 1; Table 1). Surface water at Stn 4 (7.7°C, 33.4 PSU) was cooler and less saline than the bottom water (199 m; 12°C, 35.6 PSU; Table 1). Based on water mass characteristics and previous physical oceanographic studies conducted in these waters, Stn 4 surface water was Mid Atlantic Bight shelf water, while Stn 4 bottom water originated from a Gulf Stream warm core ring. At Stn 8, surface water (18.8°C, 36.3 PSU) was characteristic of Gulf Stream water. Bottom water (4500 m) at Stn 8 measured at 2.2°C and 34.9 PSU, indicative of North Atlantic Deep Water.

Bacterial parameters and dissolved organic carbon

Initial cell counts in unamended mesocosms from all water masses showed lowest values ($3.1 \times 10^4 \pm 1.3 \times 10^4$ cells ml^{-1}) in Stn 8 surface water and highest values ($2.6 \times 10^5 \pm 6.0 \times 10^4$ cells ml^{-1}) at Stn 8 bottom water (Fig. 2A). Following HMW-OM addition (ca. 25 mg l^{-1} dry weight; 658 μM total C addition; see *Experimental Procedures*), cell numbers generally increased, and were always significantly higher than in the unamended mesocosms (ANOVA, $p < 0.022$ for all; Supporting

Table 1. Water mass physicochemical characteristics and experimental details.

	Stn 4		Stn 8	
	Surface	Bottom	Surface	Bottom
Sampling Date	28 April, 15	28 April, 15	29 April, 15	29 April, 15
Latitude (° N)	40.07	40.07	37.60	37.60
Longitude (° W)	71.00	71.00	68.40	68.40
Depth (m)	1	199	6	4574
Temperature (°C)	7.7	12.0	18.8	2.2
Salinity (PSU)	33.4	35.6	36.3	34.9
Oxygen (ml l^{-1})	7.3	4.7	5.1	5.7
DOC (μM)	103.9	71.7	73.6	43.7
Meso. Incub. Temp. (°C)	4	4	21	4
EEA Incub. Temp. (°C)	8	12	21	4

'DOC' stands for dissolved organic carbon concentration. 'Meso. Incub. Temp.' stands for mesocosm incubation temperature. 'EEA Incub. Temp' stands for extracellular enzymatic activity assay incubation temperature.

Information Table S1A). The greatest change occurred in Stn 4 bottom water amended mesocosms, in which cell counts increased by two orders of magnitude by 8 days, but decreased after this timepoint (Fig. 2A). Bacterial carbon production, measured using ^{3}H-leucine, was also significantly higher in amended mesocosms than in untreated controls (Fig. 2B; Supporting Information - Table S1A), with the exception of Stn 8 surface waters (ANOVA, $p = 0.220$). In amended mesocosms, bacterial production was highest in Stn 4 bottom water at 28 days. In contrast, bacterial production was comparatively low at Stn 8 bottom water amended mesocosms, reaching only half of the maximum bacterial production rate of Stn 4 amended bottom water (Fig. 2B). Addition of HMW-OM caused a significant increase in dissolved organic carbon (DOC) concentrations (of ca. 40–60 μM) at all stations and depths (Fig. 2C; ANOVA, $p < 0.003$ for all, Supporting Information Table S1A).

Bacterial community composition

Distinct bacterial communities characterized the different water masses, evident as separate clusters based on Bray–Curtis dissimilarities of bacterial OTUs at 97% sequence similarity (Fig. 3A). Differences between initial bacterial communities were statistically significant (ANOSIM, $R = 0.915$, $p = 0.001$; Supporting Information - Table S2). This pattern was also evident when phylogenetic distances were considered using unweighted UniFrac (Supporting Information Fig. S2A and B). On broad taxonomic levels, surface water communities were initially characterized by large relative proportions of class *Alphaproteobacteria* and *Flavobacteria*, with lesser contributions of class *Gammaproteobacteria* and phylum *Actinobacteria* (Fig. 3C). Stn 4 bottom waters showed a large relative contribution of class *Alphaproteobacteria*, followed by class *Gammaproteobacteria*, *Flavobacteria*,

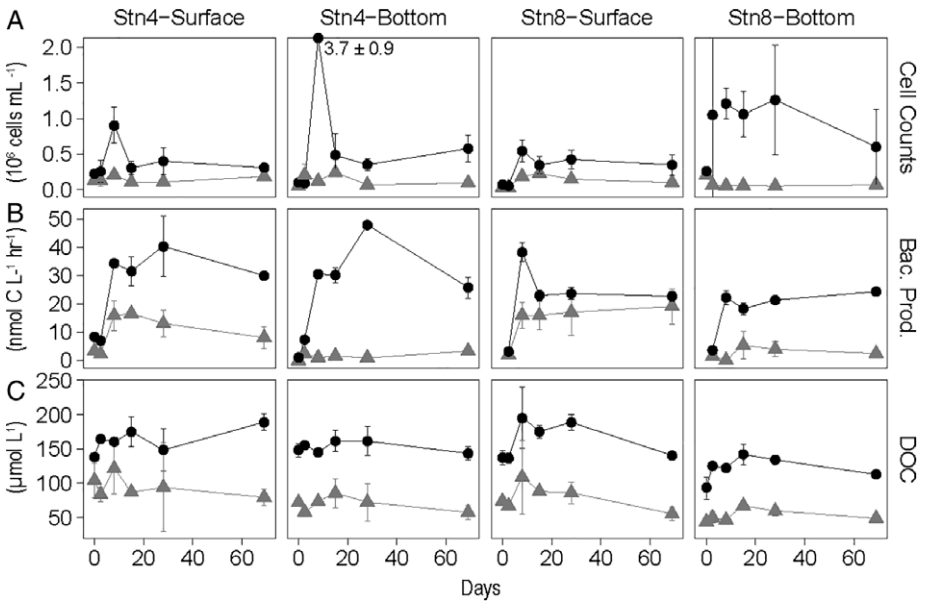

Fig. 2. Bacterial cell counts (A), ^{3}H-Leucine bacterial carbon production (B) and dissolved organic carbon (DOC) concentrations (C).
Note the differences in scale and units. Circles and triangles correspond to amended and unamended measurements, respectively; error bars show standard deviation of triplicate mesocosms.

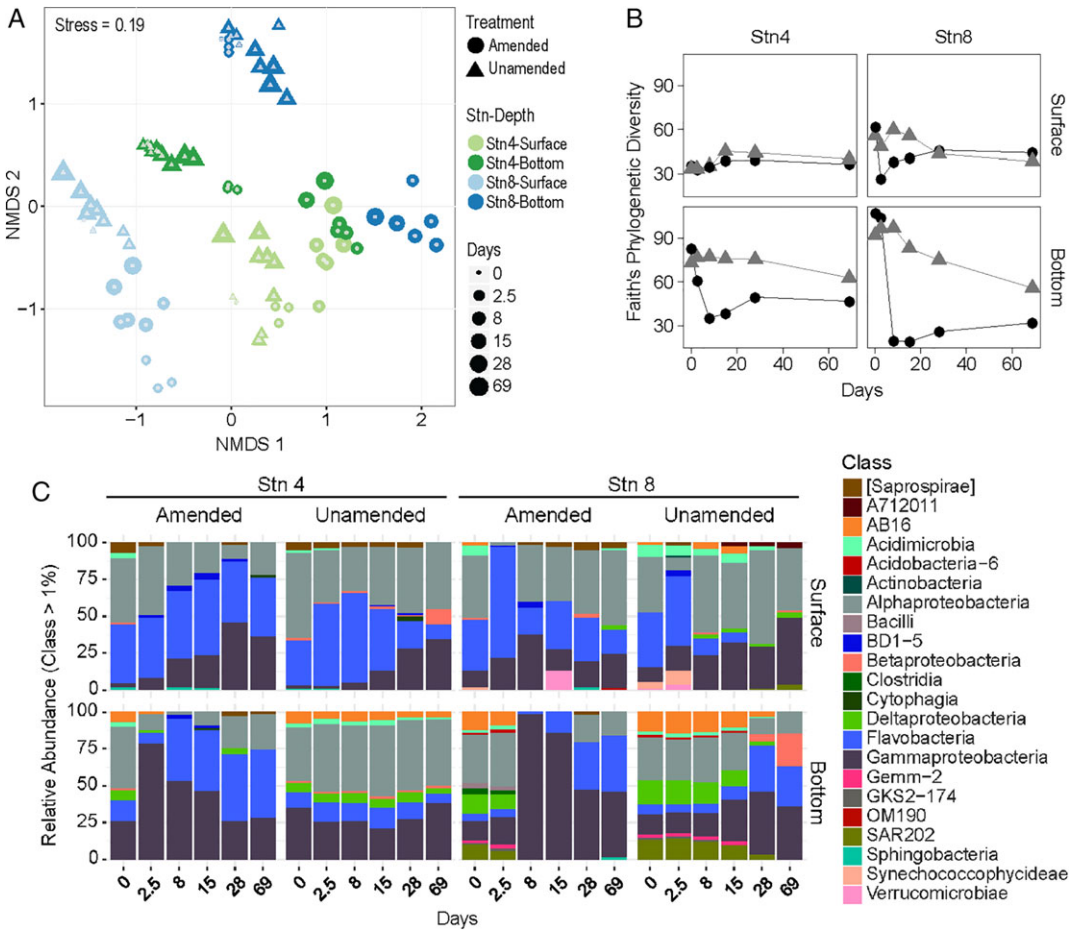

Fig. 3. Nonmetric multidimensional scaling (NMDS) of bacterial community compositional dissimilarity using Bray–Curtis index (A). The ordination was conducted on OTUs defined at 97% sequence similarity from all samples, and the distances on the NMDS are correlated with Bray–Curtis distances (Spearman correlation = 0.831, p = 0.001). Comparison of Faith's Phylogenetic Diversity index across station and depth (B). Diversity was calculated from bacterial communities from only one unamended and one amended mesocosm across all timepoints and at all locations. Circle and triangle data points correspond to amended and unamended measurements, respectively. Class-level taxonomic breakdown of bacterial communities in amended and unamended treatments (C). The visualized data are based on one unamended and one amended mesocosm from each water mass across all timepoints, as in (B). To de-convolute the plot, only bacterial classes that are ≥ 1% in relative proportions were included in the visualization.

Deltaproteobacteria and class AB16 within the phylum *Marinimicrobia* (previously classified as SAR406). Stn 8 bottom waters contained many of the same bacterial groups in similar relative proportions as Stn 4 bottom waters, but with the additional contribution of SAR202 within phylum *Chloroflexi* (Fig. 3C).

Incubation with HMW-OM altered the composition of initially distinct bacterial assemblages (Fig. 3A; Supporting Information Table S2). Changes in diversity in response to HMW-OM – calculated using Faith's phylogenetic diversity index (see *Experimental Procedures*) – varied across water masses, and ranged from a significant reduction in diversity in Stn 4 and Stn 8 bottom waters, to no change in Stn 4 surface waters (Fig. 3B; Supporting Information - Table S1A). Bacterial communities in each amended mesocosm shifted toward greater compositional (Bray–Curtis-based; Fig. 3A and C) and phylogenetic similarity (UniFrac-based; Supporting Information Fig. S2A and B) with initial and unamended bacterial communities in Stn 4 surface waters (see *Experimental Procedures* regarding compositional vs. phylogenetic similarity). However, the nature and rate of compositional shifts varied substantially by station and depth (Fig. 3B and C): whereas bacterial assemblages in amended Stn 4 surface waters exhibited incremental changes, those in other mesocosms showed more rapid and intense shifts at varying timepoints (Fig. 3A–C; Supporting Information Fig. S2). Amended mesocosms with Stn 4 bottom waters and Stn 8 surface waters exhibited robust changes by 2.5 days, while Stn 8 bottom waters only showed notable shifts at 8 days. Water mass origin of microbial communities in amended and unamended mesocosms was the largest source of community dissimilarity (PerMANOVA, R^2 = 0.314, p = 0.001), evident in the ordination space as separate

clusters by station and depth (Fig. 3A; Supporting Information Fig. S2) that differed significantly from each other (Supporting Information Table S2).

The majority of taxa that increased in the amended and unamended mesocosms belonged to the three most relatively abundant classes – *Gammaproteobacteria*, *Flavobacteria* and *Alphaproteobacteria* – but their proportions and temporal distribution varied across locations (Fig. 3C). In Stn 4 surface waters, members of the class *Gammaproteobacteria* gradually increased in relative abundances. Gammaproteobacterial taxa in the bottom waters of Stns 4 and 8 dominated in response to the treatment, albeit at differing timescales. Taxa within the class *Flavobacteria* exhibited a rapid 'boom and bust' in Stn 8 surface waters. Members of the class *Alphaproteobacteria* initially decreased in relative proportions but returned to pre-disturbance relative proportions in later timepoints (Fig. 3C).

The identities and relative contributions of specific OTUs that responded to the HMW-OM addition varied by location and treatment. Moreover, in most of these cases, the OTUs that proliferated were either undetected or only represented a minor fraction of the initial bacterial community. Within the *Gammaproteobacteria*, members of the families *Colwelliaceae*, *Moritellaceae*, *Oceanospirillaceae, Pseudoalteromonadaceae* and *Vibrionaceae* were among the immediate and most relatively abundant responders to HMW-OM addition (Supporting Information Figs S3A–E and S6C). Within these bacterial families, one or few OTUs became proportionally dominant. For example, one *Colwelliaceae* OTU dominated the amendment mesocosms from the surface water of Stn 4 and the bottom waters of Stns 4 and 8. Two different, but closely related OTUs of *Colwelliaceae* were proportionally abundant in Stn 8 surface water amended mesocosms (Supporting Information Fig. S3A). The dominant *Moritellaceae* OTU (Supporting Information Fig. S3B) exhibited a distribution pattern similar to that of the *Colwelliaceae* OTUs: abundant in the amended surface waters of Stn 4, and the amended mesocosms of Stns 4 and 8 bottom waters. Within *Pseudoalteromonadaceae*, one OTU became highly represented in the bottom waters of Stns 4 and 8 (Supporting Information Fig. S3D).

Temporal changes in the relative contribution of the class *Flavobacteria* were most rapid and robust in Stn 8 surface waters and were more gradual elsewhere, but compositional changes – usually a dominance of distinct members within the family *Flavobacteraceae* – were observed at all stations and depths. In Stn 8 surface waters, one OTU comprised the largest flavobacterial contribution; another closely related OTU increased to a lesser extent in the amended mesocosms (Supporting Information Fig. S4). Consistent with gammaproteobacterial patterns, many of the OTUs that increased in representation in the amended mesocosms were detected minimally, if at all, in the initial community composition.

In response to HMW-OM enrichment, members of the class *Alphaproteobacteria* decreased in relative abundance in the initial stages of the community development. In tandem with the decrease in relative abundance of *Alphaproteobacteria*, a compositional shift was observed (Supporting Information Fig. S5). Initially, the alphaproteobacterial communities in all water masses featured a nearly even representation of members of *Pelagibacteraceae* – dominated by an OTU most closely related to *Pelagibacter ubique* – and *Rhodobacteraceae*; following the addition of HMW-OM, the alphaproteobacterial community became dominated by OTUs within *Rhodobacteraceae.* The composition and temporal succession of *Rhodobacteraceae* OTUs, however, differed between the stations and depths (Supporting Information Fig. S5). For example, in Stn 4 surface waters, an OTU detected in moderate proportions in the initial community increased in relative contribution and became the dominant *Rhodobacteraceae* OTU. However, in Stn 8 surface water amended mesocosms, OTUs within *Rhodobacteraceae* that were initially present in moderate proportions were nearly undetectable 2.5 days after HMW-OM addition; thereafter, a distinct set of OTUs within *Rhodobacteraceae* that were undetected at the start of the incubation became dominant (Supporting Information Fig. S5).

Peptidase and glucosidase activities

Initial peptidase and glucosidase activities differed by station and depth. Activities in Stn 4 surface water were characterized initially by a large relative contribution of leucine-aminopeptidase, with lesser activities of AAPF-chymotrypsin (AAPF-chym), QAR-trypsin (QAR-tryp), FSR-trypsin (FSR-tryp) and minimal contribution of β-glucosidase activities (β-glu; Supporting Information Fig. S7A). In comparison, Stn 4 bottom water showed relatively higher proportions of AAPF-chym, with some contribution of QAR-tryp, FSR-tryp and lower contribution of β-glu (Supporting Information Fig. S7B). In Stn 8 surface water, enzymatic activities initially were relatively even (Supporting Information Fig. S7C), while in Stn 8 bottom waters, enzymatic activities were dominated by the contribution of AAF-chym (Supporting Information Fig. S7D). Summed initial rates were highest in surface waters at both stations. Over time, peptidase and glucosidase rates in unamended incubations remained low and generally showed a gradual decrease (Supporting Information Fig. S7A–D). The only exception to this general pattern were enzymatic activities in unamended mesocosms with Stn 8 surface waters, where activities of some enzymes peaked at 15 days (Supporting Information Fig. S7C), and in unamended

Stn 8 bottom waters, where AAF-chym activities increased at 2.5 days (Supporting Information Fig. S7D).

Changes in peptidase and glucosidase activities in amended mesocosms (Fig. 4) were concurrent with robust community composition shifts (Fig. 3). Within 2.5 days of HMW-OM addition, increased enzymatic activities were measured in all amended mesocosms, with the exception of those from Stn 8 bottom waters, for which a substantial increase in activity was first measured at 8 days (Fig. 4). All peptidase and glucosidase rates were significantly higher in amended versus unamended mesocosms, regardless of station and depth (ANOVA, $p < 0.05$ for all; Supporting Information - Table S1B). Furthermore, the temporal succession and highest rates of enzymatic activities were also station and depth-dependent. For many of the enzyme activities – including α-glucosidase, β-glucosidase, AAPF-chym, QAR-tryp and FSR-tryp – maximum rates were measured

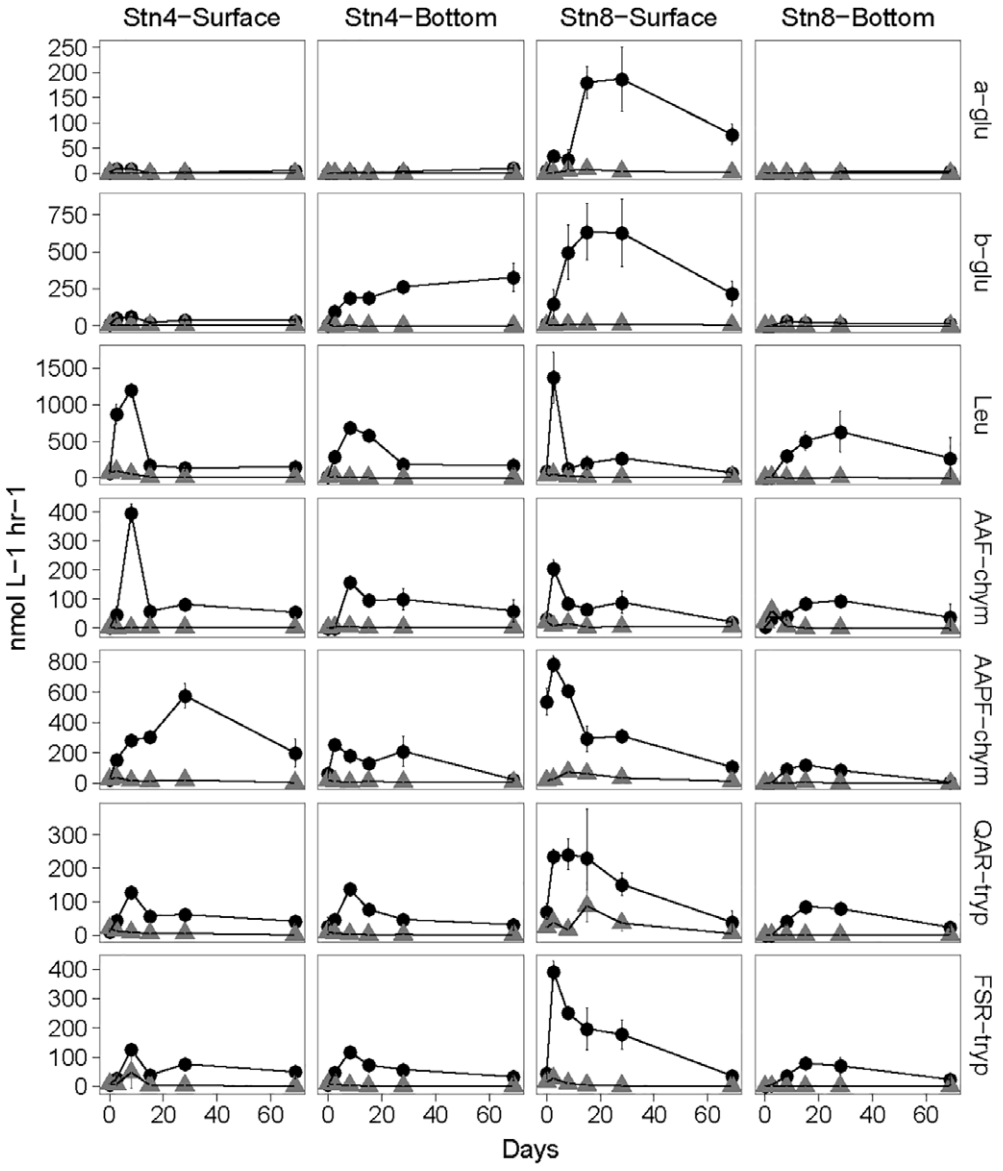

Fig. 4. Glucosidase (two upper rows) and peptidase (five bottom rows) activities at all locations.
Circles and triangles correspond to amended and unamended measurements, respectively. Each data point above shows the averaged rates and standard deviations for the triplicate amended and unamended mesocosms. For each timepoint t0–t5 (0 days–69 days), a timecourse of measurements was made with the plate reader. The rates shown here are the average of all rates obtained at each timepoint throughout the timecourse of plate incubation (see *Experimental Procedures*). Error bars indicate the standard deviation of the rate across the mesocosm triplicates. Note the scale differences among substrates on the *Y*-axis. a-glu = α = glucosidase, b-glu = β-glucosidase, Leu = Leucine, AAF-chym = Alanine–Alanine–Phenylalanine-chymotrypsin, AAPF-chym = Alanine–Alanine–Proline–Phenylalanine-Chymotrypsin, QAR-Tryp = Glutamine–Alanine–Arginine–trypsin, FSR-tryp = Phenylalanine–Serine–Arginine–Trypsin.

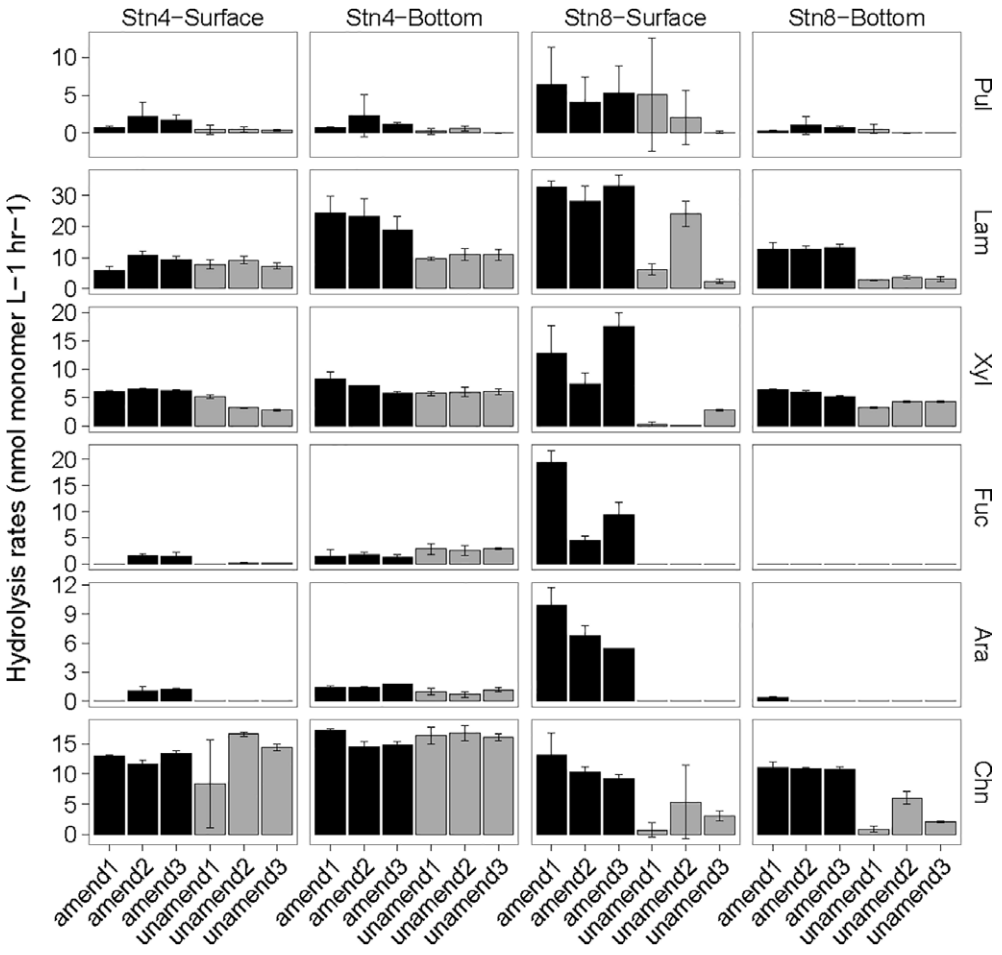

Fig. 5. Maximum polysaccharide hydrolase rates for each mesocosm.
These maximum rates were taken at varying timepoints in the polysaccharide hydrolase assays (see Supporting Information Fig. S8). The plotted rates and error bars represent the average and standard deviation of rates obtained from triplicate incubations for each mesocosm incubation (carboy). Initial water samples used for the polysaccharide hydrolase measurements were obtained at the 15 days (t3) mesocosm subsampling timepoint. Note that the timepoints for the mesocosms are different from the timepoints for the polysaccharide hydrolase assays (see *Experimental Procedures*). Pul = Pullulan, Lam = Laminarin, Xyl = Xylan, Fuc = Fucoidan, Ara = Arabinogalactan, Chn = Chondroitin.

in Stn 8 surface waters (Fig. 4). However, maximum rates of leucine aminopeptidase activities at Stn 4 surface waters were similar to those at Stn 8 surface waters, although the former was measured at 8 days, while the latter was detected at 2.5 days. In contrast, maximum rates for AAF-chym activities across all water masses were measured at Stn 4 surface waters. Surprisingly, maximum activities for most of the enzymes in Stn 8 bottom waters were comparable to those in Stn 4 bottom waters, despite differences in temperature (*in situ*, as well as incubation) and initial cell counts.

Polysaccharide hydrolase activities

Addition of HMW-OM also correlated with changes in polysaccharide hydrolase activities in all locations, but to varying degrees (Fig. 5). In amended mesocosms, all six substrates were ultimately hydrolyzed, except in Stn 8 bottom water, in which only four substrates were hydrolyzed (Fig. 5). The corresponding unamended mesocosms showed either fewer (Stns 4 and 8 surface waters) or the same (Stns 4 and 8 bottom) substrates hydrolyzed. The maximum rates (Fig. 5) and temporal development of polysaccharide hydrolase activities in amended mesocosms (Supporting Information Fig. S8) also differed between water masses (Supporting Information Table S1C). For example, pullulan was hydrolyzed at all four locations, but the highest hydrolysis rates were at Stn 8 surface water (Fig. 5). The same pattern was evident for laminarin, but with less difference in maximum rates across the water masses. Xylan was hydrolyzed at all locations at comparable rates, except for Stn 8 surface water, but the timepoints at which maximum hydrolysis was detected varied across locations: fucoidan and arabinogalactan were not hydrolyzed in Stn 8 bottom waters, and were hydrolyzed at a later timepoint

and at low rates in Stn 4 surface and bottom waters, but were rapidly hydrolyzed in Stn 8 surface waters (Supporting Information Fig. S8). Maximum rates of chondroitin hydrolysis were comparable across water masses, and in Stn 4 surface and bottom waters, these rates did not vary between amended and unamended mesocosms. Thus, the addition of HMW-OM affected enzymatic activities in ways specific to each bacterial community.

Discussion

We hypothesized that in response to HMW-OM, distinct microbial assemblages would exhibit varying compositional and functional succession, and a greater potential to produce a broader range of enzymes than indicated by initial enzyme activities. Among different bacterial communities that populate discrete water masses (e.g., Mid Atlantic Bight shelf water, Gulf Stream warm core ring, Gulf Stream and North Atlantic Deep Water), successional patterns showed similar (convergent) as well as divergent features, illustrating the complexity in interpreting the functional consequences of compositional differences (Bier *et al.,* 2015). Several initially rare taxa showed convergent patterns of proportional dominance across water masses, during which a wider range of enzyme activities were also measured. However, bacterial responses to the same pool of HMW-OM diverged substantially with regards to the timing and intensity of shifts in whole-community structure, diversity and enzymatic activities. Moreover, while a wider spectrum of enzyme activities was detectable during community succession, the types of enzymes that were stimulated (peptidases, glucosidases and/or polysaccharide hydrolases) varied between communities. Consequently, the extent to which functional differences were observed among microbial assemblages depended on the specific enzyme activity that was measured. Thus, the level of compositional and functional resolution that is considered (e.g., individual taxon vs. whole community; individual enzyme activity vs. a broad spectrum of enzymatic activities) partially influences interpretations of whether variations in community composition yield functional differences (Balser and Firestone, 2005; Langenheder *et al.,* 2006).

Conditionally rare taxa drive convergent features of compositional and functional succession

Addition of even moderate amounts of HMW-OM (25 mg l^{-1} total dry mass, ca. 658 μM total C addition) to different water masses served as an ecological filter, likely selecting for microbial taxa with the ability to metabolize particulate organic matter. A few taxa within several families of *Gammaproteobacteria*, *Alphaproteobacteria* and *Flavobacteria* dominated in the amended mesocosms (Fig. 3C). Many of these responsive taxa were closely related to each other (i.e., different OTUs within the same family, or different families within the same class), and were initially rare or undetected. Increased rates and spectra of enzyme activities characterized amended mesocosms from all locations (Figs 4 and 5, Supporting Information Figs S7 and S8) and co-occurred with the predominance of initially rare taxa within specific families of the *Gammproteobacteria*, *Alphaproteobacteria* and *Flavobacteria* (Supporting Information Figs S3–S5). Many of these bacteria are presumably copiotrophic, conditionally rare taxa (Shade *et al.,* 2014) and possess genetic repertoires – including a wider range of extracellular enzymes (Lauro *et al.,* 2009) – that enable rapid exploitation of pulses of organic matter (Newton and Shade, 2016). The boom and bust patterns of these taxa in our amended mesocosms are congruent with temporal succession patterns exhibited by conditionally rare copiotrophs (Shade *et al.,* 2014; Alonso-Sáez *et al.,* 2015; Newton and Shade, 2016). Given their dominance in amended mesocosms, these conditional members of the rare biosphere (Sogin *et al.,* 2006) likely play a major role in the degradation of sporadically available HMW-OM. In accordance with our findings, specific taxa within these bacterial classes have been observed to predominate during the course of naturally occurring phytoplankton blooms, and possess extensive hydrolytic capabilities and membrane transporters necessary to access high molecular weight substrates (Teeling *et al.,* 2012; Buchan *et al.,* 2014; Teeling *et al.,* 2016), consistent with our interpretation of their role in HMW-OM degradation.

The widespread detection and dominance of closely related taxa in response to HMW-OM highlights potential interactions of environmental selection and geographic dispersal in determining community structure and functional capabilities. For example, within *Gammaproteobacteria*, individual OTUs belonging to the families *Colwelliaceae* and *Moritellaceae* were consistently detected in high proportions in Stn 4 surface and bottom waters, as well as Stn 8 bottom water (Supporting Information Fig. S3A and B). The 'high dispersal' concept maintains that organisms are not geographically bound, but viable populations exist under favourable conditions (Darling *et al.,* 2007; Sexton and Norris, 2008). Hence, the observation that closely related taxa – and some identical OTUs (97% sequence similarity) – emerged from discrete water masses and became proportionally dominant suggests two important points. First, some microbial taxa may overcome dispersal limitation imposed by hydrographic or other physical barriers (Spencer-Cervato and Thierstein, 1997; Galand *et al.,* 2010). Oceanic dispersal of diverse plankton has been shown (Sexton and Norris, 2008; Malviya *et al.,* 2016;

Whittaker and Rynearson, 2017); however, such large vertical range – from surface waters to the bathypelagic realm – for the same taxon is not well-documented, but has been observed among taxa associated with large sinking particles (Mestre *et al.,* 2018). A second important point is that deep sea microbes may hydrolyze components of HMW-OM at rates comparable to those observed in much shallower waters (Figs 4 and 5). This finding is consistent with our hypothesis that greater potential for OM degradation exists beyond that reflected by the initial spectrum of active enzymes. Sinking particulate matter could possibly transport (Boetius *et al.,* 2013; Mestre *et al.,* 2018; Rapp *et al.,* 2018) and sustain heterotrophic microbes in the deep ocean (Nagata *et al.,* 2000; Hansell and Ducklow, 2003).

Phylogenetically narrow niche for HMW-OM degradation

The relatively narrow phylogenetic distribution of taxa that became proportionally dominant in response to HMW-OM (Fig. 3B and C) may be linked to the trait complexity of accessing this material. Trait complexity, in this context, is related to the repertoire of genes necessary to carry out specific processes (Martiny *et al.,* 2013). The ability to access particulate matter is contingent upon particle encounter rates, microbial chemotaxis and perhaps also production of exopolysaccharides to attach to surfaces (Dang and Lovell, 2016; Datta *et al.,* 2016). Accessing and metabolizing carbon sources from particulate matter requires production of appropriate enzymes that initiate hydrolysis to smaller constituents, and transporters for product uptake. In aquatic systems, the ability to degrade HMW-OM is limited to a minor fraction of the natural community (Berlemont and Martiny, 2016), whereas low molecular weight organic matter is available to a wider fraction of a community (Logue *et al.,* 2016). Moreover, initial colonizers of model particles among marine microbial taxa are also limited to those that can secrete hydrolytic enzymes (Datta *et al.,* 2016; Enke *et al.,* 2018), consistent with observations that trait complexity and its phylogenetic distribution are inversely correlated (Martiny *et al.,* 2013). The narrow niche for HMW-OM degradation also likely underlies the remarkable reproducibility in community composition (Supporting Information Fig. S6A–D) and enzymatic activities (Fig. 5, Supporting Information Fig. S7A–D) observed among triplicate mesocosms. Experiments in which LMW-OM were provided to different bacterial communities exhibited markedly different succession from each other, as well as large inter-replicate variability (Langenheder *et al.,* 2006), most likely because a wider range of taxa were able to respond to the LMW-OM (Logue *et al.,* 2016). The reproducibility of our results across triplicate mesocosms support the idea that these observed compositional and functional changes are due to the HMW-OM addition, as opposed to shifts only due to bottle effects (Stewart *et al.,* 2012).

Divergent elements of compositional and functional succession indicate functional dissimilarity

In spite of some convergent successional patterns driven by several conditionally rare taxa, many features of the compositional and functional succession – when evaluated on the whole-community level – differed considerably across communities. Bacterial diversity in amended mesocosms (1) dramatically changed in Stn 8 bottom waters, (2) were altered to a lesser extent in Stn 8 surface waters and Stn 4 bottom waters, and (3) remained similar in Stn 4 surface waters (Fig. 3B). Variations in the intensity of bacterial community diversity shifts between stations and depths likely reflect the initial differences in the number of taxa capable of occupying the HMW-OM enriched niche. To an extent, temperature may have played a role in the varied responses, although its influence is not straightforward (see Supporting Information *Text* for an expanded discussion). Moreover, the extent of community shifts may be linked to the degree of similarity of the new, perturbed environment to the ambient environment. Stn 4 surface waters typically experience high levels of primary production (Kuring *et al.,* 1990), whereas open ocean bottom waters receive a small fraction of OM exported from surface waters (Karl *et al.,* 2012). The most substantial physicochemical change after HMW-OM, relative to initial conditions, may have been at Stn 8 bottom water, based on compositional shifts and greatest bacterial diversity decrease.

Community succession in amended mesocosms were congruent with changes in enzymatic activities (Figs 4 and 5, Supporting Information Figs S7A–D and S8), vividly demonstrating the point that community composition can have robust functional consequences (Teeling *et al.,* 2012; Datta *et al.,* 2016), particularly for rates of HMW-OM degradation (Enke *et al.,* 2018). Spatiotemporal variability in enzymatic activities across amended mesocosms illustrate the nuanced responses of distinct microbial communities, characteristic of functional dissimilarity (Reed and Martiny, 2007; Strickland *et al.,* 2009) and supporting our hypothesis that community structural differences influence microbial degradation of HMW-OM. For example, HMW-OM addition resulted in substantially varied glucosidase responses between some communities (Fig. 4). The high activities of α- and β-glucosidase in amended treatments were only observed in Stn 4 bottom waters and in Stn 8 surface water. Endo-acting peptidases with distinct substrate specificities also provide a finer resolution on functional differences between microbial assemblages. The activities of the two chymotrypsins, which target different

amino acid residues attached to alanine, varied consider-ably from each other in maximum rates as well as timing of changes in Stns 4 and 8 surface waters. In contrast, the activities of the two trypsins were distinct across the water masses, but exhibited more similarity to each other with regard to maximum rates and temporal succession relative to the two chymotrypsins (Fig. 4).

Other variations in the timescales of compositional and functional shifts further highlight the differences in response between communities. Whereas substantial compositional and enzymatic activity changes were observed at 2.5 days at most locations, microbial responses were not observed in amended 4500 m waters until 8 days. Although temperature can influence enzyme kinetics, the effect of temperature is nonlinear: amended mesocosms with Stn 4 surface and bottom waters showed community compositional shifts at an earlier timepoint than those with Stn 8 bottom waters (Figs 3–5), despite being incubated at the same temperature (4°C; Supporting Information Table 1). Moreover, enzymatic activities at Stn 4 surface waters (incubated at 8°C) reached higher rates compared to those at Stn 4 bottom waters (incubated at 12°C), indicating that temperature alone cannot account for the temporal and intensity variations of microbial responses (Fig. 4). Delayed microbial response in amended 4500 m waters, relative to that in other mesocosms (Figs 3 and 4), may reflect the time period necessary to ramp up metabolism to exit dormancy – a strategy employed by microbes under energy limitations, as in deep waters, to maintain a viable population that can respond to pulses of available resources (Lennon and Jones, 2011). As a caveat, other factors that may have influenced the timing and intensity of these compositional and enzymatic responses – and which have implications for HMW-OM degradation – cannot be discounted. These factors include differences in top-down control by grazers and viruses, and in bottom-up controls by DOC, nutrients, trace elements and unmeasured physicochemical variables across water masses. Nevertheless, the robust community shift that co-occur with changes in enzymatic activities suggest that differences in community composition (Enke *et al.,* 2018) and related properties – potentially including microbial dormancy – played a major role in shaping the varied microbial responses to HMW-OM.

Measurement of a different class of enzymes, responsible for the cleavage of polysaccharides, also illustrates variations in maximum hydrolysis rates and enzyme spectra (Fig. 5) among compositionally distinct communities (Fig. 3). These findings further substantiate our hypothesis of functional dissimilarity, and suggest that polysaccharide components of HMW-OM are differentially hydrolyzed by dissimilar microbial communities. Amended waters used for polysaccharide hydrolase activity measurements were collected at the 15 days timepoint; thus, the communities that were tested for polysaccharide hydrolase activities had sufficient time to respond to the HMW-OM. Hence, the absence of detectable fucoidan and arabinogalactan hydrolysis in Stn 8 bottom water (Fig. 5) may be due to a lack of organisms enzymatically equipped to hydrolyze these substrates, related to the low community diversity observed in these waters following HMW-OM amendment (Fig. 3B and C). Alternatively, these taxa may have been present, but unable to produce the necessary hydrolytic enzymes. Similar to differences in peptidases and glucosidases, incubation temperature by itself is an unlikely reason for the lack of detectable fucoidan and arabinogalactan hydrolysis, considering that hydrolysis of these polysaccharides has been observed in low-temperature sediments of Svalbard fjords (Teske *et al.,* 2011), which were also incubated at 4°C. Thus, community-related differences most likely drove the variations in polysaccharide hydrolase activities between communities.

Conclusion

Alongside shifts in enzymatic spectra, bacterial communities exhibited substantial restructuring in response to HMW-OM. These changes were driven largely by several closely related taxa that emerged from different water masses, suggesting a role for members of microbial seed banks in cycling HMW compounds. These few taxa appear to drive a convergent response among distinct communities. However, integrating the whole-community compositional and functional succession following HMW-OM addition demonstrates robust differences across water masses. Differences in the timing, intensity and spectrum of active enzymes in response to HMW-OM suggest that the quantity and type of substrates that were consumed, or that may have evaded degradation, considerably differed among distinct communities. These results demonstrate an important consequence of community structure – bacterial functional dissimilarity for HMW-OM degradation – and indicate that spatial variations in the rate and extent of this biogeochemical process may be partially attributed to differences in bacterial community composition.

Experimental procedures

Water collection and characteristics

Between April 28 and April 29, 2015, aboard R/V *Endeavor* (EN556), seawater was collected from the surface and near bottom at two stations: one within the continental shelf of the North Atlantic (Stn 4) and the other in the open North Atlantic (Stn 8; Fig. 1). A 30 l Niskin bottle

rosette was used to collect the water. From each depth, 20 l seawater from single Niskin bottles was dispensed using acid-cleaned silicon tubing into a single polysterene (Nalgene) 20 l carboy. Prior to filling, carboys were rinsed 3x with water from the same Niskin bottle used to fill the carboy. Six carboys were filled at each depth. Samples were stored up to 12 h either at 4°C or 21°C (the incubation temperatures available aboard ship) prior to mesocosm setup.

Preparation of HMW-OM

Thalassiosira weissflogii (ReedMariculture) was frozen at −20°C, then thawed, homogenized with a tissue grinder and dialyzed using a 10 kD membrane (SpectraPor) in order to remove low molecular weight compounds. HMW dissolved OM, as well as particulate matter, were retained by the membrane. The retentate was lyophilized, autoclaved, frozen and lyophilized again. The total carbohydrate content of the added HMW-OM was 6.15%, and the C:N ratio was 6.05:1, based on an average C content of 316 333 ppm and N content of 52 266 ppm across triplicates.

Mesocosm setup and subsampling

Triplicate 20 l carboys were amended with ca. 25 mg l^{-1} dry weight of HMW-OM (exact mass was recorded for each addition); unamended triplicate carboys were used as controls. Assuming that 31.6% of 25 mg l^{-1} HMW-OM was C (based on C:N content described previously), the amount of C added to the amended mesocosms was 658 μM C (dissolved and particle organic carbon). All mesocosms were incubated in the dark: Stn 8 surface water mesocosms were stored at room temperature (ca. 21°C), while the rest were kept at 4°C. Due to limited temperature ranges and/or space constraints in incubators/cold rooms aboard the ship, the mesocosm incubation temperatures (Meso. Incub. Temp, Table 1) differed from the extracellular enzymatic activity assay incubation temperatures (EEA Incub. Temp, Table 1) for Stn 4, as described below. Mesocosms were subsampled at the start of incubation, and then after 2.5 days, 8 days, 15 days, 28 days and 69 days for the following assays: bacterial protein production using ^{3}H-leucine, DOC, nutrients, bacterial cell counts, peptidase and glucosidase activity measurements and bacterial community composition analyses. At the 15 days timepoint, subsamples were also collected to begin the incubations to measure polysaccharide hydrolase activities. Because the added HMW-OM presumably contained substrates that differed in bioavailability, microbial responses may occur over a wide range of timescales (hours to months). Given that, *a priori*, the timescales of response were unknown, we extended the experimental window to 69 days to increase the likelihood that we could also captured microbial responses occurring on very extended timescales.

Bacterial protein production and cell counts

Bacterial protein production was measured in triplicate, plus a killed control. Each live replicate and killed control received 1.5 ml of mesocosm water and L-[3,4,5-3H(N)]-Leucine (PerkinElmer, NET460250UC), to a final concentration of 20 nM; the killed control additionally received 100% (w/v) TCA. Samples were incubated between 4 h and 24 h in the dark, close to *in situ* temperature and then killed using 89 μl of 100% TCA. Incorporated radioactivity was measured using an LSA scintillation counter (PerkinElmer Tri-CARB 2910TR). Samples were processed following previously established protocols (Kirchman *et al.,* 1985; Kirchman, 2001). Leucine incorporation rates were converted to bacterial protein production (BPP) following the conversion equation by Simon and Azam (1989):

$$BPP\,(g) = (mol\,leucine_{inc})\,x\,1797\,x\,ID$$

We used an isotope dilution (ID) = 1 for a conservative estimate and because the isotope dilution factor is unknown in our study. BPP was subsequently converted to bacterial carbon production (BCP) by multiplying to 0.86 (Simon and Azam, 1989; Kirchman, 2001).

Bacterial cells were counted by flow cytometry (Gasol and del Giorgio, 2000). At each subsampling timepoint, 1 ml sample water was fixed with 0.1% glutaraldehyde (final concentration) for 10 min at room temperature in the dark, and stored frozen at −80°C. Prior to analysis, thawed samples were pipetted through a cell strainer (Flowmi, 70 μm porosity) and stained with SYBR Green I for 15 min on ice in the dark. Counts were performed with a FACSCalibur flow cytometer (Becton-Dickson) using fluorescent microspheres (Molecular Probes) of 1 μm in diameter as internal size standard. Cells were counted according to their right angle scatter and green fluorescence using the FloJo 7.6.1 software.

DOC concentration

Subsamples were filtered through a combusted glass fibre filter (GFF, Whatman 1825-025 Glass Microfiber Binder Free Filter) in a polycarbonate filter holder attached to a 60 cc syringe. The filtrate was collected in 20 ml scintillation vials and acidified with 100 μl of 50% phosphoric acid. Acidified samples were frozen at −20°C until analysis via high temperature catalytic oxidation on a Shimadzu Total Organic Carbon analyser (TOC-8000A/5050A).

Peptidase and glucosidase activities

Activities of exo- (terminal-unit cleaving) and endo-acting (mid-chain cleaving) peptidases and exo-acting glucosidases were measured using methylcoumarin-labelled (MCA) peptide and methylumbelliferyl-tagged (MUF) glucose substrates: leucine-MCA (Leu), alanine–alanine–phenylalanine-MCA (AAF-chym), alanine–alanine–proline–phenylalanine-MCA (AAPF-chym), glutamine–alanine–arginine-MCA (QAR-tryp), boc-phenylalanine–serine–arginine (FSR-tryp), α-D-glucopyranoside (α-glu) and β-D-glucopyranoside (β-glu). At each timepoint, from each amended and unamended mesocosm, live and autoclaved (killed control) seawater was added to 200 μl 96-well plates (black, 'U' bottom, polystyrene). For each mesocosm, each enzyme activity was measured in triplicate. Peptide and glucose substrates were added to a final concentration of 125 μM, a concentration chosen following an initial saturation curve and kept constant for all enzymatic assays. Fluorescence was measured over a timecourse of 72 h using a plate reader (Tecan Spectra-Fluor Plus). Fluorescence values were converted to concentration of hydrolyzed substrate by comparison with a standard curve made from the fluorescence response of free MCA and MUF. Assays for peptidases and glucosidases – as well as polysaccharide hydrolases (described below) – were incubated at temperatures close to ambient water temperature, but which differed from those for the mesocosm incubations for Stn 4 surface and bottom waters (Table 1) due to space limitations.

Polysaccharide hydrolase activities

Activities of enzymes that hydrolyze six polysaccharides – pullulan, laminarin, xylan, fucoidan, arabinogalactan and chondroitin sulfate – were measured using fluorescently labelled (FLA-) polysaccharides incubated in mesocosm waters subsampled at the 15 days (t3) timepoint, as previously described (Arnosti, 2003). Polysaccharide hydrolase activity was measured in the mesocosm water 15 days post-HMW-OM addition in order to give the microbial community time to react – via changes in enzyme expression or community composition – to the addition of HMW-OM. Given the length of time required to measure polysaccharide hydrolase activities (incubation times of days to weeks) as well as the time-consuming nature of sample analysis, we did not measure polysaccharide hydrolase activities in the seawater initially added to the carboys. Polysaccharide incubations were carried out at *in situ* temperature and subsampled immediately after FLA-polysaccharide addition, and at timepoints 2 days, 5 days, 10 days, 17 days, 30 days and 62 days post-addition; note that the polysaccharide hydrolase incubation timepoints are separate and different from the mesocosm timepoints. The effect of treatment on enzymatic activities, as well as other bacterial parameters, including bacterial cell counts, bacterial production, enzymatic activities and DOC was tested using Analysis of Variance (ANOVA), considering a split-plot design with the mesocosm replicates as random variables. We report the maximum rates in the main text to focus on the maximum potentials of the community, but the hydrolysis rates measured at all timepoints are included in the Supporting Information (Fig. S8).

DNA extraction, sequencing, community composition and statistical analyses

Samples were filtered using a vacuum pump through a 0.2 μm pore size 47 mm diameter Whatman Nucleopore track-etched membrane filter for DNA extractions. The volumes filtered ranged from 300 ml to 1 l, depending on cell densities. Filters were stored at −80°C until DNA extraction. For community analysis, only a subset of all samples was sequenced. These included all timepoint samples from the first amended and unamended (amend1 and unamend1) replicate mesocosms. For biological replication, samples from the second and third amended and unamended (amend2, amend3, unamend2 and unamend 3) replicate mesocosms were also analysed at 2.5 days (t1) and 15 days (t3; Supporting Information Fig. S6A–D). A Powersoil DNA extraction kit (Qiagen) was used to extract DNA following manufacturer protocol. The V1-V2 hypervariable region of the 16S rRNA gene was amplified and sequenced using Illumina MiSeq PE 2x250 and the following primer set at the UNC Core Microbiome Sequencing Facility: 8F (5′- AGA GTT TGA TCC TGG CTC AG -3′) and 338R (5′- GCT GCC TCC CGT AGG AGT -3′).

Sequenced amplicon pairs were merged using Fastq-join on QIIME (Caporaso *et al.,* 2010), and the quality of the merged reads were evaluated using FastQC. Any sequences with a mean Phred score below 24 were excluded from downstream analyses. OTUs at the 97% sequence similarity cutoff were picked *de novo* using QIIME. Chimeric sequences – identified using *ChimeraSlayer* (Haas *et al.,* 2011) – and singletons were also excluded from further analyses. Greengenes was used for OTU taxonomic classification (DeSantis *et al.,* 2006). The BIOM-formatted OTU table and phylogenetic tree of representative sequences were used as input for downstream analysis using *phyloseq* library on R Studio (McMurdie and Holmes, 2013). Data used for whole-community analyses were rarefied (random subsampling without replacement) to 22,000 sequences per sample to enable comparison of bacterial relative proportions across samples with initially uneven sequencing depths.

Raw sequence files are available on NCBI Sequence Read Archive under the accession number SRP148429.

To explore differences in bacterial community composition, Bray–Curtis (compositional) dissimilarity indices were calculated for each community, and were ordinated using Nonmetric multidimensional scaling (NMDS). An NMDS and PCoA (Principal Coordinates Analysis) ordination were also performed using unweighted UniFrac (phylogenetic) dissimilarity indices (Lozupone and Knight, 2005), and are available in the Supporting Information (Fig. S2A and B). Briefly, the unweighted UniFrac dissimilarity index takes into consideration phylogenetic (16S-based) distances between taxa, whereas the Bray–Curtis dissimilarity index does not. Differences in community similarity using the Bray–Curtis index were then tested using Analysis of Similarity (ANOSIM; Supporting Information Table S2). Permutational multivariate analysis of variance (PerMANOVA), as implemented through 'adonis' on the R package *vegan* (Oksanen *et al.,* 2013) was used to quantify the variation in community dissimilarities (Bray–Curtis) as a function of water mass origin. Community diversity was measured using Faith's Phylogenetic Diversity index (Faith, 1992) – which calculates the branch lengths that connect different taxa in a pre-computed phylogenetic tree – as implemented on the R package *picante* (Kembel *et al.,* 2010).

Acknowledgements

We thank the captain, crew and scientific party of R/V *Endeavor* (EN556) for their fieldwork support. Additionally, we thank Karylle Abella-Hall for assistance with sample processing, Dr. Jakub Kwintikiewicz for sequencing assistance, and Jeff Roach for advice with sequence processing. We thank Dr. John Bane for advice on the physical oceanography, and Dr. Barbara MacGregor and Dr. Ronnie Glud for comments on the manuscript as it appeared in JPB's thesis. We also thank the anonymous reviewers, whose thoughtful comments considerably improved the manuscript. This project and JP Balmonte were funded by NSF OCE-1332881 and OCE-1736772 to Carol Arnosti. JP Balmonte was additionally funded by a UNC Dissertation Completion Fellowship.

References

Agogue, H., Lamy, D., Neal, P. R., Sogin, M. L., and Herndl, G. J. (2011) Water mass-specificity of bacterial communities in the North Atlantic revealed by massively parallel sequencing. *Mol Ecol* **20**: 258–274.

Allison, S. D., and Martiny, J. B. H. (2008) Resistance, resilience, and redundancy in microbial communities. *Proc Natl Acad Sci USA* **105**: 11512–11519.

Alonso-Sáez, L., Díaz-Pérez, L., and Morán, X. A. G. (2015) The hidden seasonality of the rare biosphere in coastal marine bacterioplankton. *Environ Microbiol* **17**: 3766–3780.

Arnosti, C. (2003) Fluorescent derivatization of polysaccharides and carbohydrate-containing biopolymers for measurement of enzyme activities in complex media. *J Chromatogr B* **793**: 181–191.

Arnosti, C. (2011) Microbial extracellular enzymes and the marine carbon cycle. *Ann Rev Mar Sci* **3**: 401–425.

Azam, F., and Malfatti, F. (2007) Microbial restructuring of marine ecosystems. *Nat Rev Microbiol* **5**: 782–791.

Balmonte, J. P., Teske, A., and Arnosti, C. (2018) Structure and function of high Arctic pelagic, particle-associated, and benthic bacterial communities. *Environ Microbiol* **20**: 2941–2954.

Balser, T. C., and Firestone, M. K. (2005) Linking microbial community composition and soil processes in a California annual grassland and mixed-conifer forest. *Biogeochemistry* **73**: 395–415.

Baltar, F., Aristegui, J., Sintes, E., van Aken, H. M., Gasol, J. M., and Herndl, G. J. (2009) Prokaryotic extracellular enzymatic activity in relation to biomass production and respiration in the meso- and bathypelagic waters of the (sub)tropical Atlantic. *Environ Microbiol* **11**: 1998–2014.

Bell, T., Newman, J. A., Silverman, B. W., Turner, S. L., and Lilley, A. K. (2005) The contribution of species richness and composition to bacterial services. *Nature* **436**: 1157–1160.

Berlemont, R., and Martiny, A. C. (2016) Glycoside hydrolases across environmental microbial communities. *PLoS Comput Biol* **12**: e1005300. https://doi.org/10.1371/journal.pcbi.1005300.

Bier, R. L., Bernhardt, E. S., Boot, C. M., Graham, E. B., Hall, E. K., Lennon, J. T., *et al*. (2015) Linking microbial community structure and microbial processes: an empirical and conceptual overview. *FEMS Microbiol Ecol* **91**: fiv113.

Boetius, A., Albrecht, S., Bakker, K., Bienhold, C., Felden, J., Fernandez-Mendez, M., *et al*. (2013) Export of algal biomass from the melting Arctic Sea ice. *Science* **339**: 1430–1432.

Buchan, A., LeCleir, G. R., Gulvik, C. A., and Gonzalez, J. M. (2014) Master recyclers: features and functions of bacteria associated with phytoplankton blooms. *Nat Rev Microbiol* **12**: 686–698.

Burke, C., Thomas, T., Lewis, M., Steinberg, P., and Kjelleberg, S. (2011) Composition, uniqueness and variability of the epiphytic bacterial community of the green alga *Ulva australis*. *ISME J* **5**: 590–600.

Caporaso, J. G., Kuczynski, J., Stombaugh, J., Bittinger, K., Bushman, F. D., and Costello, E. K. (2010) QIIME allows analysis of high-throughput community sequencing data. *Nat Methods* **7**: 335–336.

Christian, J. R., and Karl, D. M. (1995) Bacterial ectoenzymes in marine waters: activity ratios and temperature responses in three oceanographic provinces. *Limnol Oceanogr* **40**: 1042–1049.

Comte, J., Fauteux, L., and del Giorgio, P. A. (2013) Links between metabolic plasticity and functional redundancy in freshwater bacterioplankton communities. *Front Microbiol* **4**: 112.

D'Ambrosio, L., Ziervogel, K., MacGregor, B., Teske, A., and Arnosti, C. (2014) Composition and enzymatic function of

particle-associated and free-living bacteria: a coastal/offshore comparison. *ISME J* **8**: 2167–2179.

Dang, H., and Lovell, C. R. (2016) Microbial surface colonization and biofilm development in marine environments. *Microbiol Mol Biol Rev* **80**: 91–138.

Darling, K. F., Kucera, M., and Wade, C. M. (2007) Global molecular phylogeography reveals persistent Arctic circumpolar isolation in a marine planktonic protist. *Proc Natl Acad Sci USA* **104**: 5002–5007.

Datta, M. S., Sliwerska, E., Gore, J., Polz, M. F., and Cordero, O. X. (2016) Microbial interactions lead to rapid micro-scale successions on model marine particles. *Nat Commun* **7**: 11965.

Davey, K. E., Kirby, R. R., Turley, C. M., Weightman, A. J., and Fry, J. C. (2001) Depth variation of bacterial extracellular enzyme activity and population diversity in the northeastern North Atlantic Ocean. *Deep Sea Res II* **48**: 1003–1017.

DeSantis, T. Z., Hugenholtz, P., Larsen, N., Rojas, M., Brodie, E. L., Keller, K., *et al*. (2006) Greengene, a chimera-checked 16S rRNA gene database and work-bench compatible with ARB. *Appl Environ Microbiol* **72**: 5069–5072.

Enke, T. N., Leventhal, G. E., Metzger, M., Saavedra, J. T., and Cordero, O. X. (2018) Microscale ecology regulates particulate organic matter turnover in model marine microbial communities. *Nat Commun* **9**: 2743. https://doi.org/10.1038/s41467-018-05159-8.

Faith, D. P. (1992) Conservation evaluation and phylogenetic diversity. *Biol Conserv* **61**: 1–10.

Frossard, A., Gerull, L., Mutz, M., and Gessner, M. O. (2012) Disconnect of microbial structure and function: enzyme activities and bacterial communities in nascent stream corridors. *ISME J* **6**: 680–691.

Fukuda, R., Sohrin, Y., Sotome, N., Fukuda, H., Nagata, T., and Koike, I. (2000) East-west gradient in ectoenzyme activities in the subarctic Pacific: possible regulation by zinc. *Limnol Oceanogr* **45**: 930–939.

Galand, P. E., Potvin, M., Casamayor, E. O., and Lovejoy, C. (2010) Hydrography shapes bacterial biogeography of the deep Arctic Ocean. *ISME J* **4**: 564–576.

Gasol, J. M., and del Giorgio, P. A. (2000) Using flow cytometry for counting natural planktonic bacteria and understanding the structure of planktonic bacterial communities. *Sci Mar* **64**: 28.

Haas, B. J., Gevers, D., Earl, A. M., Feldgarden, M., Ward, D. V., Giannoukos, G., *et al*. (2011) Chimeric 16S rRNA sequence formation and detection in sanger and 454-pyrosequenced PCR amplicons. *Genome Res* **21**: 494–504.

Hansell, D. A., and Ducklow, H. W. (2003) Bacterioplankton distribution and production in the bathypelagic ocean: directly coupled to particulate organic carbon export? *Limnol Oceanogr* **48**: 150–156.

Hartley, B., Barber, H. G., Carter, J. R., Sims, P. A. (1996) *An atlas of British diatoms*. Bristol: Biopress Ltd.

Hoarfrost, A., and Arnosti, C. (2017) Heterotrophic extracellular enzymatic activities in the Atlantic Ocean follow patterns across spatial and depth regimes. *Front Mar Sci* **4**: 200. https://doi.org/10.3389/fmars.2017.00200.

Karl, D. M., Church, M. J., Dore, J. E., Letelier, R. M., and Mahaffey, C. (2012) Predictable and efficient carbon sequestration in the North Pacific Ocean supported by symbiotic nitrogen fixation. *Proc Natl Acad Sci USA* **109**: 1842–1849.

Kembel, S. W., Cowan, P. D., Helmus, M. R., Cornwell, W. K., Morlon, H., Ackerly, D. D., *et al*. (2010) R tools for integrating phylogenies and ecology. *Bioinformatics* **26**: 1464–1464.

Kirchman, D. (2001) Measuring bacterial biomass production and growth rates from leucine incorporation in natural aquatic environments. *Method Microbiol* **30**: 227–237.

Kirchman, D., K'Nees, E., and Hodson, R. (1985) Leucine incorporation and its potential as a measure of protein synthesis by bacteria in natural aquatic systems. *Appl Environ Microbiol* **49**: 599–607.

Knelman, J. E., and Nemergut, D. R. (2014) Changes in community assembly may shift the relationship between biodiversity and ecosystem function. *Front Microbiol* **5**: 424.

Kuring, N., Lewis, M. R., Platt, T., and O'Reilly, J. E. (1990) Satellite-derived estimates of primary production on the Northwest Atlantic continental shelf. *Cont Shelf Res* **10**: 461–484.

Langenheder, S., Lindström, E. S., and Tranvik, L. J. (2006) Structure and function of bacterial communities emerging from different sources under identical conditions. *Appl Environ Microbiol* **72**: 212–220.

Lauro, F. M., McDougald, D., Thomas, T., Williams, T. J., Egan, S., Rice, S., *et al*. (2009) The genomic basis of trophic strategy in marine bacteria. *Proc Natl Acad Sci USA* **106**: 15527–15533.

Lennon, J. T., and Jones, S. E. (2011) Microbial seed banks: the ecological and evolutionary implications of dormancy. *Nat Rev Microbiol* **9**: 119–130.

Louca, S., Polz, M. F., Mazel, F., Albright, M. B. N., Huber, J. A., O'Connor, M. I. *et al*. (2018) Function and functional redundancy in microbial systems. *Nat Ecol Evol* **2**(6): 936–943.

Logue, J. B., Stedmon, C. A., Kellerman, A. M., Nielsen, N. J., Andersson, A. F., Laudon, H., *et al*. (2016) Experimental insights into the importance of aquatic bacterial community composition to the degradation of dissolved OM. *ISME J* **10**: 533–545.

Lozupone, C., and Knight, R. (2005) UniFrac: a new phylogenetic method for comparing microbial communities. *Appl Environ Microbiol* **71**: 8228–8235.

Malviya, S., Scalco, E., Audic, S., Vincent, F., Veluchamy, A., Poulain, J., *et al*. (2016) Insights into global diatom distribution and diversity in the world's ocean. *Proc Natl Acad Sci USA* **113**: E1516–E1525.

Martiny, A. C., Treseder, K., and Pusch, G. (2013) Phylogenetic conservatism of functional traits in microorganisms. *ISME J* **7**: 830–838.

McMurdie, P. J., and Holmes, S. (2013) Phyloseq: an R package for reproducible interactive analysis and graphics of microbiome census data. *PLoS One* **8**: e61217.

Mestre, M., Ruiz-González, C., Logares, R., Duarte, C. M., Gasol, J. M., and Sala, M. M. (2018) Sinking particles promote vertical connectivity in the ocean microbiome. *Proc Natl Acad Sci USA* **115**: E6799–E6807. https://doi.org/10.1073/pnas.1802470115.

Nagata, T., Fukuda, H., Fukuda, R., and Koike, I. (2000) Bacterioplankton distribution and production in deep Pacific waters: large-scale geographic variations and possible coupling with sinking particle fluxes. *Limnol Oceanogr* **45**: 426–435.

Newton, R. J., and Shade, A. (2016) Lifestyles of rarity: understanding heterotrophic strategies to inform the ecology of the microbial rare biosphere. *Aquat Microb Ecol* **78**: 51–63.

Oksanen, J., Blanchet, F. G., Kindt, R., Legendre, P., Minchin, P. R., O'Hara, R. B., *et al*. (2013). Vegan: Community Ecology Package (R package versions 2.0-10). http://vegan.r-forge.r-project.org/

Rapp, J. Z., Fernández-Méndez, M., Bienhold, C., and Boetius, A. (2018) Effects of ice-algal aggregate export on the connectivity of bacterial communities in the Central Arctic Ocean. *Front Microbiol* **9**:1035. doi: 10.3389/fmicb.2018.01035.

Reed, H. E., and Martiny, J. B. H. (2007) Testing the functional significance of microbial composition in natural communities. *FEMS Microbiol Ecol* **62**: 161–170.

Sexton, P. F., and Norris, R. D. (2008) Dispersal and biogeography of marine plankton: long-distance dispersal of the foraminifer *Truncorotalia truncatulinoides*. *Geology* **36**: 899–902.

Shade, A., Jones, S. E., Caporaso, J. G., Handelsman, J., Knight, R., Fierer, N., *et al*. (2014) Conditionally rare taxa disproportionately contribute to temporal changes in microbial diversity. *mBio* **5**(4):e01371–14. doi: 10.1128/mBio.01371-14

Simon and Azam (1989) Protein content and protein synthesis rates of planktonic marine bacteria. *Miar Ecol Prog Ser* **51**:201–213.

Sogin, M. L., Morrison, H. G., Huber, J. A., Welch, D. A., Huse, S. M., Neal, P. R., *et al*. (2006) Microbial diversity in the deep sea and the underexplored "rare biosphere.". *Proc Natl Acad Sci USA* **103**: 12115–12120.

Spencer-Cervato, C., and Thierstein, H. R. (1997) First appearance of *Globorotalia truncatulinoides*: cladogenesis and immigration. *Mar Micropaleontol* **30**: 267–291.

Steen, A. D., Vazin, J. P., Hagen, S. M., Mulligan, K. H., and Wilhelm, S. W. (2015) Substrate specificity of aquatic extracellular peptidases assessed by competitive inhibition assays using synthetic substrates. *Aquat Microb Ecol* **75**: 271–281.

Stewart, F. J., Dalsgaard, T., Young, C. R., Thamdrup, B., Revsbech, N. P., Ulloa, O., *et al*. (2012) Experimental incubations elicit profound changes in community transcription in OMZ bacterioplankton. *PLoS One* **7**: e37118.

Stoermer, E. F. (1978) TPhytoplankton assemblages as indicators of water quality in the Laurentian Great Lakes. *Trans Am Microsc Soc.* **97**(1): 2–16.

Strickland, M. S., Lauber, C., Fierer, N., and Bradford, M. A. (2009) Testing the functional significance of microbial community composition. *Ecology* **90**: 441–451.

Teeling, H., Fuchs, B. M., Becher, D., Klockow, C., Gardebrecht, A., Bennke, C. M., *et al*. (2012) Substrate-controlled succession of marine bacterioplankton populations induced by a phytoplankton bloom. *Science* **336**: 608–611.

Teeling, H., Fuchs, B. M., Bennke, C. M., Krüger, K., Chafee, M., Kappelmann, L., *et al*. (2016) Recurring patterns in bacterioplankton dynamics during coastal spring algae blooms. *Elife* **5**: e11888.

Teske, A., Durbin, A., Ziervogel, K., Cox, C., and Arnosti, C. (2011) Microbial community composition and function in permanently cold seawater and sediments from an Arctic fjord of Svalbard. *Appl Environ Microbiol* **77**: 2008–2018.

Weiss, M. S., Abele, U., Weckesser, J., Welte, W., Schiltz, E., and Schulz, G. E. (1991) Molecular architecture and electrostatic properties of a bacterial porin. *Science* **254**: 1627–1630.

Whittaker, K. A., and Rynearson, T. A. (2017) Evidence for environmental and ecological selection in a microbe with no geographic limits to gene flow. *Proc Natl Acad Sci USA* **114**: 2651–2656.

Zaccone, R., Monticelli, L. S., Serriti, A., Santinelli, C., Azzaro, M., Boldrin, A., *et al*. (2003) Bacterial processes in the intermediate and deep layers of the Ionian Sea in winter 1999: vertical profiles and their relationship to the different water masses. *J Geophys Res* **108**: 8117. https://doi.org/10.1029/2002JC001625.

Supporting Information

Additional Supporting Information may be found in the online version of this article at the publisher's web-site:

Appendix S1: Supporting information